

## On the formation of deformation bands in fatigued copper single crystals

S. X. LI†, X. W. LI, Z. F. ZHANG, Z. G. WANG and K. LU

Shenyang National Laboratory for Materials Science, Institute of Metal Research, Chinese Academy of Sciences, Shenyang 110015, PR China

[Received 21 August 2001 and accepted in revised form 3 April 2002]

### ABSTRACT

The features of the deformation bands (DBs) in copper single crystals under cyclic straining were surveyed. A simple model was proposed to account for the formation of DBs. In this model, both crystal rotation and dislocation density variation induced by cyclic straining were considered. The gradual lattice rotation caused by tension and compression irreversibility is the main driving force for the formation of DBs. The drastic release of mobile dislocations resisted by the primary slip bands is the direct trigger for the formation of DBs. From this analysis, one may understand why the formation of DBs is easier in copper single crystals with double- and multiple-slip orientations than that with single-slip orientation. At the same time the effect of the dislocation avalanche factor on the formation of DBs was discussed.

### §1. INTRODUCTION

Besides the general slip bands (SBs) and the persistent slip lines (Li *et al.* 1998a, 2002) as well as the well-known persistent slip bands (PSBs) in copper single crystals, the formation of deformation bands (DBs) seems to be another important feature induced by cyclic deformation. Recently, DBs have been frequently observed in fatigued copper single crystals with various orientations. Gostelow (1971) and Mughrabi (1978) found that the DBs analogous to the kink band occurred in single-slip-oriented copper single crystals cyclically deformed at a high strain amplitude of about  $10^{-2}$ . In general, two types of DB, namely DBI and DBII, and occasionally DBIII, have been identified in fatigued copper single crystals (Saletore and Taggart 1978, Jin and Winter 1984, Li *et al.* 1994, Gong *et al.* 1995, 1997, Zhang 1995, Li *et al.* 1998b, 1999a, b, c, 2000b, Zhang *et al.* 2000), where DBI is approximately parallel to the primary slip plane, while DBII makes a certain angle with the primary slip plane.

Among many features of cyclic deformation of copper single crystals, the occurrence of DBs is probably the least understood. These DBs will disrupt an initially smooth surface of the specimen, influencing not only the process of initiation of fatigue cracks but also their subsequent direction of propagation (Saletore and Taggart 1978). Therefore, it is necessary to understand the mechanism for the formation of DBs.

---

† Email: shxli@imr.ac.cn.

The possible mechanisms for the formation of DBs in copper single crystals under cyclic straining were proposed in our previous papers. Initially, a dislocation avalanche model was proposed to explain the formation of DBs in which the variation in dislocation density was assumed to play a key role (Li *et al.* 1994). Recently, an analysis based on the crystallographic deformation geometry showed that the local irreversible rotation of a crystal which exists during symmetrical push-pull loading might be responsible for the formation of DBs (Li *et al.* 2000b). However, a reasonable model is still needed to modify the complicated mechanism for the formation of DBs.

In this paper, firstly, a survey of the formation of DBs in various orientations of copper single crystals under cyclic straining was carried out, and then a model was proposed, in which both crystal rotation and variation in dislocation density were considered.

## §2. SURVEY OF THE FORMATION OF DEFORMATION BANDS

### 2.1. *Experimental details*

The detailed experimental procedures, including the growth and preparation of the specimens of copper single crystals with various orientations as well as the symmetrically cyclic deformation testing at constant plastic shear strain amplitudes, have been given by various researchers (for example Li *et al.* (2000b)).

### 2.2. *Deformation bands in copper single crystals with various orientations*

The orientations of the copper single crystals oriented for single, double and multiple slip in which the occurrence of DBs was observed are shown in the stereographic projection in figure 1. Recently, Li *et al.* (2000b) found that the DBs denoted as DBI and DBII develop roughly along the primary slip plane  $\{111\}$  and conventional kink plane  $\{101\}$  respectively, and the habit planes of DBI and DBII are perpendicular to each other. For each single crystal investigated, the related data are shown in table 1. From this table, one can see that the indices of the DBs with different values were determined; however, if the coordinates of the crystal are rearranged, the indices of the DBs could be determined solely, that is the habit planes of DBI and DBII are close to  $(111)$  and  $(101)$  respectively. For example, for the  $[001]$  orientation, the indices of DBI  $(-0.69\ 0.57\ 0.47)$  changes to  $(0.69\ 0.57\ 0.47)$ , and DBII  $(0.74\ 0.06\ 0.66)$  to  $(-0.74\ 0.06\ 0.66)$  correspondingly. For the  $[\bar{1}17]$  orientation, the index of DBI  $(0.65\ 0.60\ 0.46)$  changes to  $(0.60\ 0.65\ 0.46)$ , and DBII  $(-0.01\ -0.63\ 0.77)$  to  $(-0.63\ -0.01\ 0.77)$ . A similar transformation can be applied to other orientations if it is needed.

On the formation of DBs, two critical plastic shear strains could be noted; that is, below the first critical shear strain  $\gamma_{pl,cI}$ , no DBs are observed and, above that, one kind of DB (DBI or DBII) can be observed; at the second critical shear strain  $\gamma_{pl,cII}$ , both DBI and DBII are observed. The data on these critical strains are also drawn in figure 1 for comparison. It should be borne in mind that these data are approximate values because intervals of the plastic shear strain amplitudes applied in the testing are sometimes rather large (in a few cases only one plastic shear strain amplitude was applied (Jin and Winter 1984)), and that some data were not recorded because, in the early work, not much attention was paid to the formation of DBs. However, some features may be pointed out as follows (since the data on  $\gamma_{pl,cI}$  are lacking, we shall pay more attention to  $\gamma_{pl,cII}$ ).

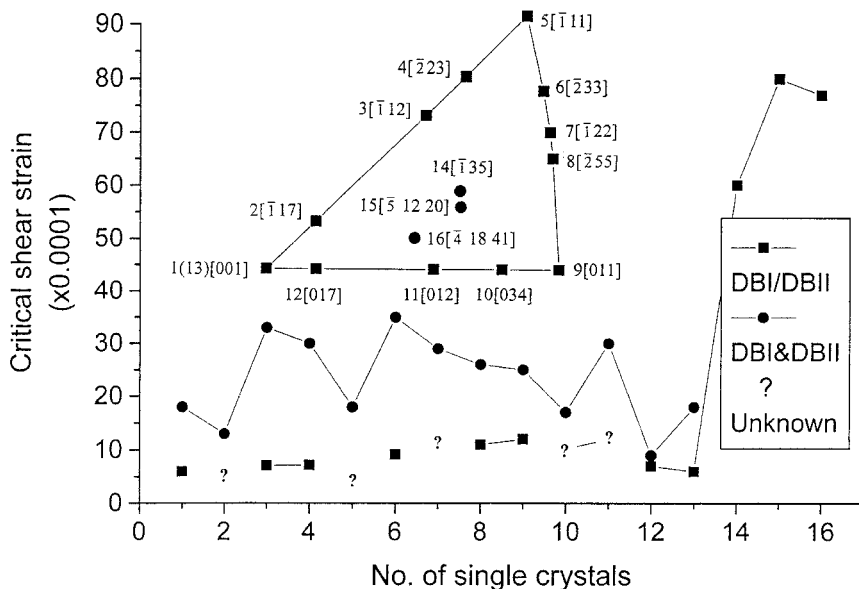


Figure 1. The critical shear strain for various orientations of copper single crystals. The inset shows the orientations investigated in the standard stereographic triangle. The different orientations are numbered as indicated in the inset. The data for the various orientations were taken from the following references: 1, Gong *et al.* (1997); 2, Gong *et al.* (1995); 3, Li *et al.* (1999c); 4, Li *et al.* (1999c); 5, Villechaise *et al.* (1991); 6, Li *et al.* (1999a); 7, Jin and Winter (1984); 8, Zhang (1995); 9, Li *et al.* (1998b); 10, Gong *et al.* (1995); 11, Jin and Winter (1984); 12, Li *et al.* (1999b); 13, Gong *et al.* (1997); 14, Li *et al.* (2000b); 15, Zhang *et al.* (2000); 16, Li *et al.* (1998b).

- (i) The critical plastic strain amplitude  $\gamma_{pl,c}$  needed for the formation of DBs is relatively smaller for double-slip or multiple-slip crystals than that for single-slip crystals. In other words, the formation of DBs in double- or multiple-slip crystals is easier than in single-slip crystals (see figure 1).
- (ii) For multiple-slip single crystals ([001], [111] and [011]), the formation of DBs for [011] needs the largest critical shear strain amplitude.
- (iii) Generally speaking, along each side of the stereographic triangle there is a wave crest of critical strains (see figure 1).
- (iv) The habit planes of DBI and DBII are close to (111) and ( $\bar{1}01$ ) respectively. They are perpendicular to each other.

### §3. A MODEL FOR THE FORMATION OF DEFORMATION BANDS

#### 3.1. The cyclic hardening curves of single crystals

##### 3.1.1. The cyclic hardening curves

The cyclic hardening curves of copper single crystals oriented for single, double and multiple slip have been well studied by numerous researchers (Mughrabi 1978, Cheng and Laird 1981, Hong and Laird 1990, Villechaise *et al.* 1991, Gong *et al.* 1995, 1997, Zhang 1995, Li *et al.* 1998b, 1999a, b, c).

Table 1. The DBs in various orientations of copper single crystals.

Orientation	Loading axis	Habit plane of DBs	Angle (degrees) between the following												$\gamma_{\text{DBI, DBII}} \times 10^{-3}$
			DBI and loading axis	DBII and loading axis	DBI and (111)	DBI and (111)	DBI and (101)	DBI and (101)	DBI and (110)	DBI and (101)	DBI and (101)	DBI and (110)	DBI and (101)	DBI and (101)	
1 (13)	[001]	DBI (-0.69 0.57 0.47) DBII (0.74 0.06 0.66)	28	41	8	8	8	6	6	99	6.0	1.8			
2	$\bar{1}$ [117]	DBI (0.65 0.60 0.46) DBII (-0.01 -0.63 0.77)	26	42	9	9	8	8	92	1.3					
3	$\bar{1}$ [112]	DBI (0.65 0.51 0.57) DBII (-0.64 -0.07 0.77)	24	59	3	3	4	4	89	7.1	3.3				
4	[223]	DBI (0.59 0.60 0.54) DBII (-0.64 -0.02 0.77)	23	59	3	3	4	4	88	7.2	3.0				
5	$\bar{1}$ [111]	DBIII (1 0 0) DBIII (0 1 0)	35 35						90	1.8					
6	[233]	DBI (0.65 0.57 0.50) DBII (-0.44 -0.25 0.86)	24	35	7	7	23	23	90	9.2	3.5				
7 <sup>a</sup>	[122]	DBI (-0.28 -0.23 0.62) DBII (0.70 -0.71 0.05)	21	42	23	23	3	3	90	2.9					
8	[255]	DBI (0.70 0.57 0.44) DBII (-0.65 0.76 0.0)	30	44	9	9	4	4	89	11	2.6				
9	[011]	DBI (0.49 0.67 0.56) DBII (-0.63 -0.18 0.76)	60	24	45	45	11	11	90	12	2.5				
10	[034]	DBI (0.54 0.64 0.56) DBII (-0.59 -0.21 0.78)	56	30	4	4	14	14	91	1.7					
11 <sup>a</sup>	[012]	DBI (0.57 0.58 0.58) DBII (-0.74 0.66 0.14)	50	25	3	3	8	8	92	3.0					

<sup>a</sup> The orientations of DBs in  $\bar{1}$ [22] and [012] were deduced from the figures in the paper by Jin and Winter (1984).

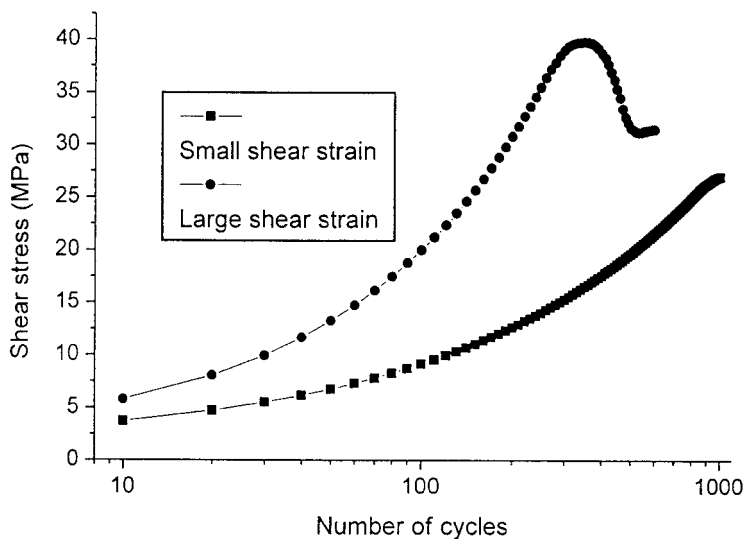


Figure 2. Schematic diagram of the cyclic strain-hardening behaviour. At larger shear strain amplitudes, cyclic softening occurs.

The characteristics of these curves might be drawn schematically as in figure 2. When the plastic shear strain amplitude is smaller, the hardening curves usually do not show a softening behaviour. When the plastic shear strain amplitude is larger, the hardening curves may show a softening behaviour (figure 2). This is particularly true for single-slip single crystals (see figure 1 of the paper by Mughrabi (1978)). Some hardening curves show rather complex behaviours; however, in the present paper, as the first approximation, it is assumed that the DBs start to form as the softening occurs.

### 3.1.2. The quantitative description of the cyclic hardening curves

Based on the model proposed by Kuhlmann-Wilsdorf and Laird (1977, 1979), the cyclic hardening curves of copper single-slip crystals in the hardening stage can be written as (Cheng and Laird 1981, Hong and Laird 1990)

$$\tau_{ps} = \tau_0 + 2B\gamma_{pl,cum}^{1/2} + a\gamma_{pl,cum}, \tag{1}$$

where  $\tau_{ps}$  is the peak shear stress,  $\gamma_{pl,cum}$  is the cumulative shear strain;  $\gamma_{pl,cum} = 4N\gamma_{pl}$ , where  $N$  is the number of cycles and  $\gamma_{pl}$  is the plastic shear strain amplitude.  $\tau_0$ ,  $B$  and  $a$  are materials constants which can be determined by experiments.

Gong *et al.* (1998) found that the hardening curves of the copper multiple-slip crystals are quite similar to those of the single-slip crystals. They can be expressed as

$$\tau_{pm} = \frac{\theta_m \gamma_{pl,m}}{\theta_s \gamma_{pl,s}} \tau_{ps} \tag{2}$$

where  $\tau_{pm}$  is the peak shear stress for multiple-slip crystals, and  $\theta_m$  and  $\theta_s$  are the hardening coefficients for multiple- and single-slip crystals respectively.  $\gamma_{pl,m}$  and  $\gamma_{pl,s}$  are plastic shear strain amplitudes for multiple- and single-slip crystals respectively.

In equation (1),  $\tau_0 = 0.8$  MPa,  $B = 4.5$  MPa and  $a = 1.15$  MPa; thus equation (1) can be approximately expressed as  $\tau_{ps} = 7.64\gamma_{pl,cum}^{0.537}$ ; therefore, for simplicity the hardening curves of the copper crystals with various orientations might be written as

$$\tau_p = A\gamma_{pl,cum}^n, \quad (3)$$

where  $\tau_p$  is the peak shear stress,  $A$  is the material constant and  $n$  is the cyclic hardening coefficient.

### 3.2. The microstructures of deformation bands

Recently, the microstructures of DBs of copper crystals have been observed using the electron channelling contrast technique in conventional scanning electron microscopy. Gong *et al.* (1997) found that the microstructure within DBs in a fatigued copper [001] crystal consists of a typical labyrinth structure. Li *et al.* (2000b) and Zhang *et al.* (2000) observed that the dislocation walls are the predominant microstructure within DBs in [135] and [5 12 20] crystals.

If the orientations of crystals are different, the microstructures of DBs are rather different. However, a lattice rotation of a few degrees between DBs and the matrix can certainly be detected in the single crystals as seen in multiple-slip [001] crystals (figure 10 of the paper by Gong *et al.* (1997)) and in single-slip [135] crystals (figure 3 of the paper by Li *et al.* (2000b)). The rotation angle between DBs and the matrix is about  $4-5^\circ$ . This can be obtained by observing the deflection of slip traces. For example, in figure 3 of present paper, a SB was disrupted by the DB into two parallel segments, denoted SBa and SBb. From the shift in the two segments and the width of the DB, a rotation angle of  $4-5^\circ$  between the DB and matrix can be estimated.

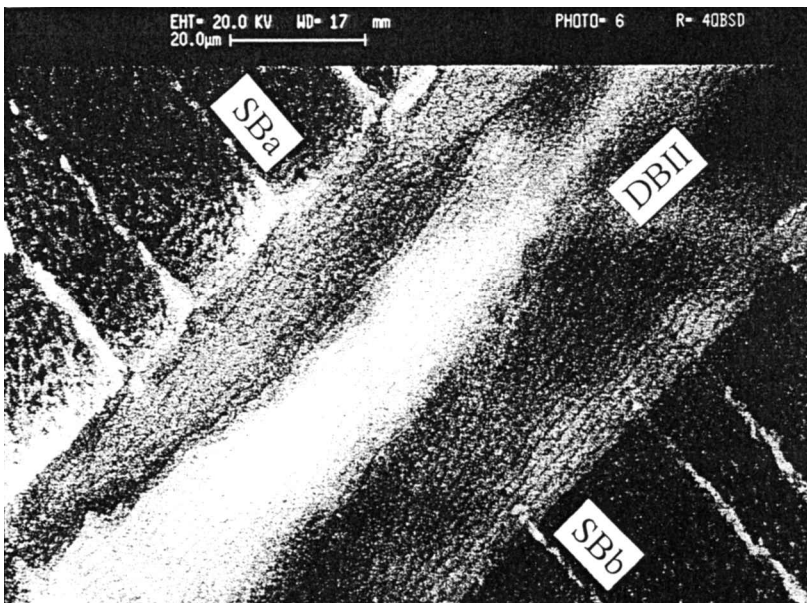


Figure 3. There is a rotation angle of about  $4-5^\circ$  between the DB and the matrix. The loading axis is [5 12 20].

By using time-resolved acoustic microscopy, Zhai *et al.* (1995, 1996) found that a lattice rotation of about  $6^\circ$  between DBs and matrix existed in a cyclically deformed aluminium single crystal.

From these observations, it seems that a lattice rotation is involved in the formation of DBs to some extent. It was revealed that the DBs formed in copper single crystals during cyclic straining might exhibit quite different microstructures, depending upon the crystallographic orientations. The difference of the dislocation microstructures of the DBs suggests that different slip systems had operated during the formation of DBs.

### 3.3. A model for the formation of deformation bands under cyclic straining

#### 3.3.1. A simple model

From the assumption mentioned above (see § 3.1) the formation of DBs arises from the cyclic softening of crystals. It is a form of plastic instability and, in symmetrically cyclic straining; the deforming zone (the cross-section of the specimen) is almost constant; therefore the condition for instability is  $d\sigma/d\varepsilon_{pl,cum} < 0$ . Here, we define  $\varepsilon_{pl,cum} = \gamma_{pl,cum}/M$ , where  $M$  is the reciprocal of the Schmid factor in single crystals.  $M$  is not a constant in fatigue testing of single crystals because the orientation changes during cycling.

For single crystals, the normal stress  $\sigma$  is related to the shear stress as  $\sigma = M\tau$ . The shear stress  $\tau$  depends on the velocity of dislocations contributing to the imposed strain rate and can be written

$$\tau = \tau_p \left( \frac{v}{v_0} \right)^m, \tag{4}$$

where  $\tau_p$  is the peak stress in each cycle,  $v$  is the dislocation velocity, which is equal to  $v_0$  when the stress is  $\tau_p$ , and  $m$  is the strain-rate sensitivity. The shear strain rate is

$$\dot{\gamma} = \rho b v, \tag{5}$$

where  $\rho$  is the density of mobile dislocations and  $b$  is the magnitude of the Burgers vector.

Substituting equations (3)–(5) into the equation  $\sigma = M\tau$ , then

$$\sigma = A(bv_0)^{-m} M^{n+1} \varepsilon_{pl,cum}^n \rho^{-m} \dot{\gamma}^m. \tag{6}$$

Since  $\gamma = M\varepsilon$  and  $\dot{\gamma} = \dot{M}\varepsilon + M\dot{\varepsilon}$ , the factor  $\dot{\gamma}^m$  in equation (6) can be written as  $(\dot{M}\varepsilon + M\dot{\varepsilon})^m$ ; however, in each cycle, the variation in  $M$ , that is  $\dot{M}$ , is very small, and  $\varepsilon$  is a small quantity; so  $\dot{M}\varepsilon$  is negligible and therefore equation (6) can be rewritten as

$$\sigma = A(bv_0)^{-m} M^{n+m+1} \varepsilon_{pl,cum}^n \rho^{-m} \dot{\varepsilon}^m. \tag{7}$$

From equation (7), the condition for instability can be derived as

$$\frac{1}{\sigma} \frac{\partial \sigma}{\partial \varepsilon_{pl,cum}} = \frac{n}{\varepsilon_{pl,cum}} + \frac{m}{\dot{\varepsilon}} \frac{\partial \dot{\varepsilon}}{\partial \varepsilon_{pl,cum}} + \frac{1+m+n}{M} \frac{\partial M}{\partial \varepsilon_{pl,cum}} - \frac{m}{\rho} \frac{\partial \rho}{\partial \varepsilon_{pl,cum}} \leq 0. \tag{8}$$

Equation (8) is quite similar to the instability criterion for the formation of shear bands formation in rolling (Dillamore *et al.* 1979), however, it is proposed for the first time for the formation of DBs in cyclic straining. In other words, the equation

given by Dillamore *et al.* (1979) can only deal with shear band formation under monotonic loading, while equation (8) can deal with the formation of DBs under cyclic loading.

During fatigue testing, in each cycle the strain rate  $\dot{\epsilon}$  is imposed by the machine; there is no substantial change in  $\dot{\epsilon}$  in consecutive cycles under constant plastic-strain-amplitude control; hence the second term on the right-hand side of equation (8) may be negligible. The condition for the formation of DBs can be rewritten as

$$\frac{n}{\epsilon_{\text{pl,cum}}} + \frac{1+m+n}{M} \frac{\partial M}{\partial \epsilon_{\text{pl,cum}}} - \frac{m}{\rho} \frac{\partial \rho}{\partial \epsilon_{\text{pl,cum}}} \leq 0. \quad (9)$$

In equation (9), the first term is always positive, therefore the last two terms are essential for the formation of DBs. In the early stage of cyclic straining, it is generally accepted that the total dislocation density increases; however, the number of mobile dislocations gradually decreases with increasing number of cycles. Hence, the last term will be positive before the formation of DBs. The second term, that is geometric softening with a negative value, will be the driving force in the formation of DBs.

### 3.3.2. Variation in the crystal orientation with cycling

Reid (1973) pointed out that, in a unidirectional tensile test, a fcc single crystal rotates in such a way that the tensile axis approaches its primary slip direction  $[\bar{1}01]$  while, in a unidirectional compressive test, the stress axis rotates towards the normal to the primary slip plane (111). Therefore, an irreversible rotation is expected in the crystal even under symmetrical tension–compression loading. As shown in figure 4,

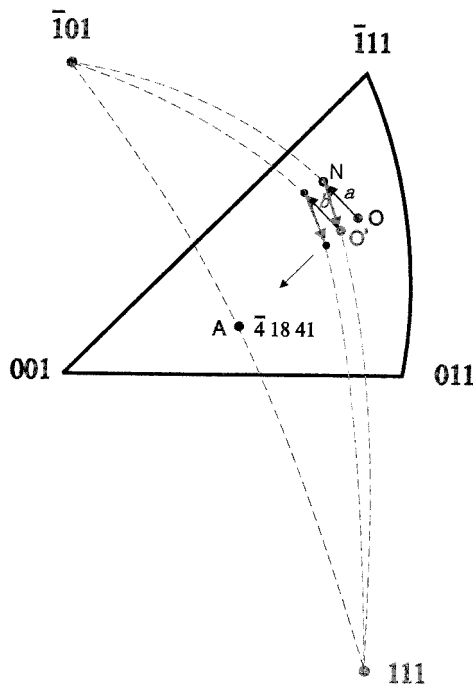


Figure 4. A stereographic projection of irreversible rotation of fcc crystal axis orientation under cyclic straining.

when a single crystal with a stress axis O is subjected to tensile loading, the stress axis of the crystal will rotate towards [101] along the great circle passing through [101] and O to N. Alternatively, when a compressive loading is applied, the current stress axis N of the crystal will move towards [111] from N to O' along the great circle through N and [111]. This irreversible rotation will be accumulated with cycling.

When a single crystal is subjected to unidirectional tension or compression, the corresponding rotational angles towards [101] or [111] can be expressed as

$$\sin \lambda = \frac{L_0}{L} \sin \lambda_0, \quad (10)$$

$$\sin \varphi = \frac{L'}{L_0} \sin \varphi_0, \quad (11)$$

where  $\lambda_0$  and  $\lambda$  are the angles between the stress axis and the primary slip direction before and after tension respectively, and  $\varphi_0$  and  $\varphi$  are the angles between the stress axis and the normal to the primary slip plane before and after compression respectively.  $L_0$  is the initial length, and  $L$  and  $L'$  are the lengths after tension and compression respectively.  $L$  and  $L'$  can be written as

$$L = L_0(1 + \gamma_{\text{pl}}\Omega), \quad (12)$$

$$L' = L_0(1 - \gamma_{\text{pl}}\Omega), \quad (13)$$

where  $\Omega$  is the Schmid factor. Based on these equations, the variation in crystal orientation with cycling can be calculated by computer. In the calculation the Schmid factor is a variable.

Taking  $\varepsilon_{\text{pl,cum}} = \gamma_{\text{pl,cum}}/M$  and  $\gamma_{\text{pl,cum}} = 4N\gamma_{\text{pl}}$ ,  $\gamma_{\text{pl}}$  is a constant in the testing, the second term of equation (9) can be rewritten as

$$\frac{1+m+n}{M} \frac{\partial M}{\partial \varepsilon_{\text{pl,cum}}} = \frac{1+m+n}{4\gamma_{\text{pl}}M} \frac{\partial M}{\partial (N/M)}. \quad (14)$$

From equations (10) to (13), the geometric softening factor  $(1/M)\partial M/\partial (N/M)$  shown in equation (14) can be calculated by computer.

The geometric softening of seven typical orientations, including three multiple-slip orientations ([001], [111] and [011]), three double-slip orientations ([112], [255] and [034]) and one single-slip orientation ([135]) were studied in detail. Since a plastic shear strain amplitude of around  $7 \times 10^{-4}$  could cause the formation of DBs, this value was chosen for calculation.

Figure 5 shows that the geometric softening factor  $(1/M)\partial M/\partial (N/M)$  varies with the cyclic number  $N$ . From these curves one can see that the absolute values of geometric softening factor for multiple-slip and double-slip single crystals are larger than that for single-slip single crystals. For example, at 1000 cycles, the softening factor for the single-slip orientation [135] is about  $-1 \times 10^{-5}$  (figure 5(a)); however, the corresponding values for multiple-slip and double-slip single crystals range from  $-4 \times 10^{-4}$  to  $-5 \times 10^{-5}$  (figure 5(b) and (c)). In other words, the driving force for the formation of DBs in the latter crystals is about an order of magnitude higher than in single-slip crystals.

Figure 6 shows the curves of the first two terms of equation (9) for the crystal orientation [112]. The values  $m = 0.7$  (Greenman *et al.* 1967) and  $n = 0.54$  were used in calculation. From this figure, one can see that the sum of the first two terms

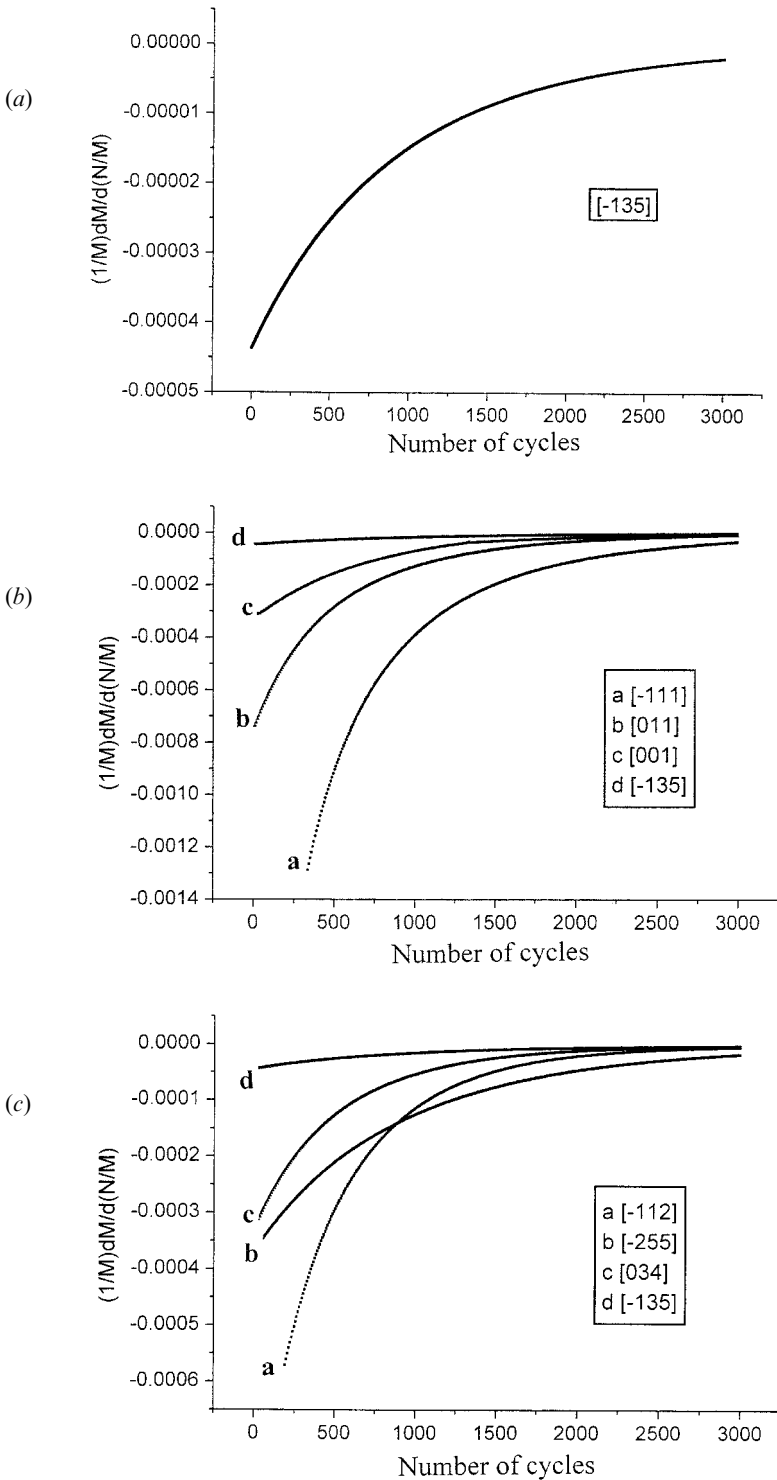


Figure 5. The values of  $(1/M)[\partial M/\partial(N/M)]$  versus number\_of\_cycles: (a) for  $[-135]$ ; (b) for  $[-135]$ ,  $[001]$ ,  $[111]$ ,  $[011]$ ; (c) for  $[-135]$ ,  $[112]$ ,  $[255]$  and  $[034]$ .

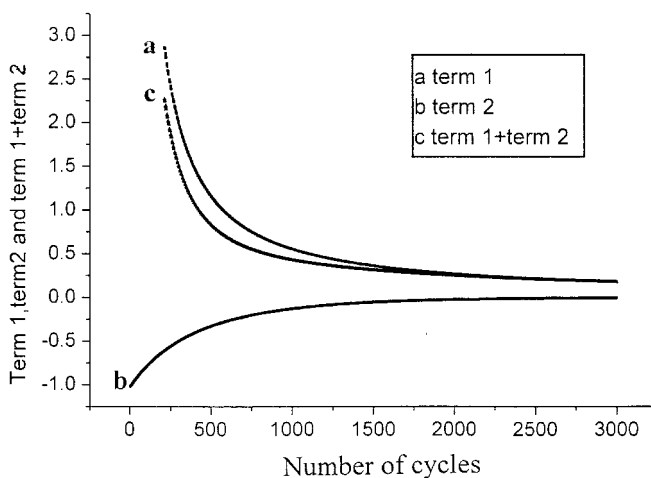


Figure 6. The values of the first and second terms and their sum in equation (9) for the  $[112]$  orientation. At 1000 cycles;  $a = 0.557$ ,  $b = -0.128$  and  $c = 0.429$ . At 2000 cycles,  $a = 0.270$ ,  $b = -0.023$  and  $c = 0.247$ .

cannot become negative easily with increasing number of cycles. The last term in equation (9) must play a decisive role in the formation of DBs.

Figure 7 shows that the rotation angle between the current and original loading axes increases under cyclic straining. The rotation angles for multiple-slip and double-slip single crystals are much larger than for single-slip single crystals. For example, at 3000 cycles, the rotation angles are  $16\text{--}30^\circ$  for multiple-slip single crystals (figure 7(a)) and  $10\text{--}18^\circ$  for double-slip single crystals (figure 7(b)), while for single-slip ( $[115]$ ) single crystals it is only about  $5^\circ$ .

Since the sample is constrained by the grips in fatigue testing, the actual rotation angles are much less than those obtained by calculation. During fatigue testing, the rotation angle is gradually increased cycle by cycle; this will cause the sample to bend and store the extra strain energy in it. It is proposed that, when the rotation angle reaches a few degrees, the bending and its strain energy will result in the formation of DBs. The DBs with a few degrees rotation accommodate the bending of the sample. At this time, the mobile dislocation density must increase drastically and the DBs start to form. There might exist a critical rotation angle above which the DBs begin to form.

From this analysis, DBI and DBII have profiles similar to those associated with tension and compression shear bands, and the orthogonality of their habit planes is therefore not surprising.

### 3.3.3. Increase in the mobile dislocation density with straining

The dislocation structures in copper single crystals have been investigated for a long time; some typical structures such as PSBs are well understood, and the dislocation structures and their related characteristics of cyclic deformation in copper single crystals with various orientations have been examined by Li *et al.* (2000c, d, 2001) recently. However, the dislocation evolution, particularly the mobile dislocation density variation at the stage of formation of DBs, has not well been studied in detail (Yang *et al.* 2001, Li *et al.* 2002).

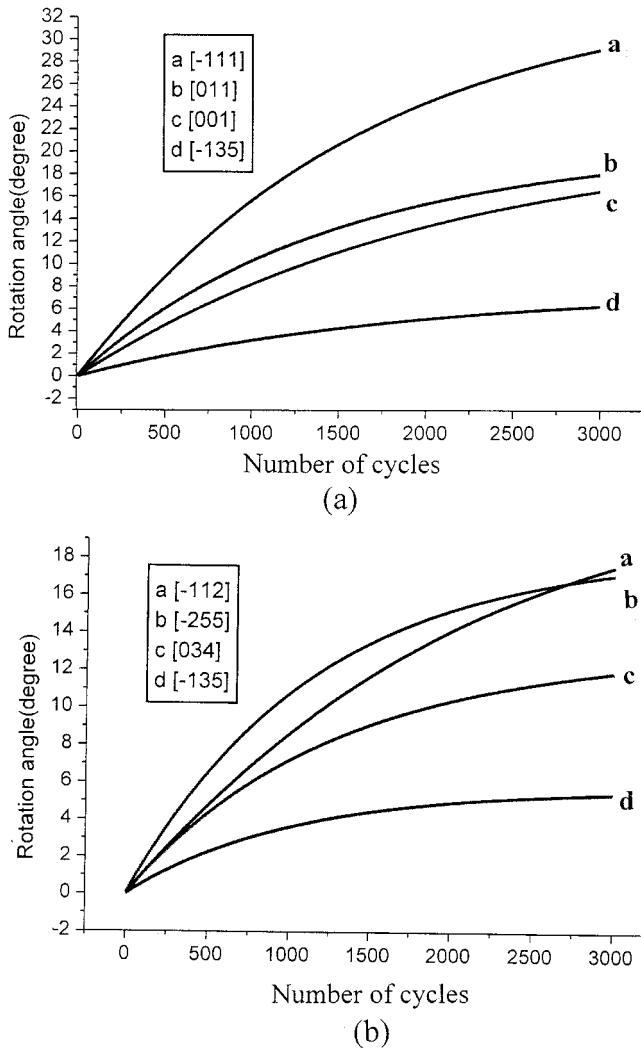


Figure 7. The rotation angles between current and initial loading axes under cyclic straining: (a) for [001], [111], [011] and [135]; (b) for [112], [255], [034] and [135].

As mentioned above, the increase in the driving force for the formation of DBs is a process of accumulating the strain energy gradually. However, when the rotation angle reaches a critical value, the formation of DBs is rather a transient process. The dislocation avalanche model (Lee and Duggan 1994, Li *et al.* 1994) could be used in the present analysis.

During cyclic deformation, the SBs or PSBs are well developed along the primary slip plane (111). When the crystal rotates gradually to a critical situation, the driving force stimulates the secondary slip system to operate. However, the slip system that intercepts the primary SBs cannot operate easily and its dislocations must be blocked at the primary SB boundaries. This is easily understood for multiple- and double-slip crystals. For single-slip crystals, the DBs occur in the range C of



where  $d\gamma_s$  and  $\Omega_s$  are the increment in shear strain and the Schmid factor of the secondary slip system respectively. The increment in shear strain can be written as

$$d\gamma_s = d\rho_{II} b OB = \frac{d\rho_{II} bf(\mathbf{s})t_2}{\cos \beta}, \quad (17)$$

where  $f(\mathbf{s})$  represents the ratio of OB to OC, and  $\mathbf{s}$  is the unit vector of the secondary slip direction (figure 8). The calculation of  $f(\mathbf{s})$  is given in appendix A.  $b$  is the magnitude of the Burgers vector.

Combining equations (15)–(17), we have

$$\frac{d\rho_{II}}{d\varepsilon_s} = \frac{1}{bf(\mathbf{s})t_2} \frac{\cos \beta}{\Omega_s}. \quad (18)$$

At the same time, some of the dislocations blocked in the primary slip plane, such as the clustered primary dislocations, for example, in the veins or the walls, could also be set free locally as secondary dislocations operate. The freed primary dislocations could form the DBI that is very close to the primary slip plane. The freed primary dislocation density is

$$d\rho_I = \frac{dN_p}{t_1 d_c}, \quad (19)$$

where  $dN_p$  is the number of blocked primary dislocations that are set free now,  $t_1$  is the thickness of DBI and  $d_c$  is a microstructure-related dimension that freed dislocations pass through. Considering that the strain  $d\varepsilon_p = \Omega_p d\gamma_p$  and  $d\gamma_p = d\rho_I b d_c$ , where  $\Omega_p$  is the Schmid factor of the primary slip system, while  $d\gamma_p$  is the shear strain caused by freed primary dislocations, then we have

$$\frac{d\rho_I}{d\varepsilon_p} = \frac{1}{b\Omega_p d_c}. \quad (20)$$

Now the last term of equation (9) can be approximately written as

$$-\frac{m}{\rho} \frac{\partial \rho}{\partial \varepsilon_{pl,cum}} \approx -\frac{m}{4Nb\rho(t_2 d_c)^{1/2}} \left( \frac{\cos \beta}{f(\mathbf{s})\Omega_p\Omega_s} \right)^{1/2}. \quad (21)$$

Here, the geometric average of  $d\rho_I/d\varepsilon_p$  and  $d\rho_{II}/d\varepsilon_s$  is used, since both factors affect the formation of DBs simultaneously. In other words, the concurrent operation of the blocked primary and secondary dislocations would result in the local crystal rotation and thus could stimulate the formation of DBs in these local regions. Also, the relation  $\varepsilon_{pl,cum} = 4N\varepsilon_{pl}$  is considered in deducing equation (21).

In equation (21), the fact that the mobile dislocation density  $\rho$  varies with the cyclic number  $N$  has not been well established in experimental and theoretical work. Therefore it is not suitable to try to deduce the detailed variation in this term with  $N$  in the present paper. However, this term may give us a hint about the formation of DBs. Therefore the order of magnitude of this term should be checked as follows.

In cyclically deformed copper single crystals, there is a higher dislocation density in the so-called wall or vein structures and it can be as high as  $10^{15}$ – $10^{16} \text{ m}^{-2}$  (Basinski *et al.* 1969). In the channels, the dislocation density is about two to three orders of magnitude smaller than in the clustered regions (Antonopoulos *et al.* 1976, Antonopoulos and Winter 1976). In the present model, the blocked dislocations are assumed to be set free which will increase the mobile dislocation

density  $d\rho$ ; at that moment, the initial mobile dislocation density  $\rho$  is mainly controlled by the dislocations in the channels. Therefore the mobile dislocation density  $\rho = 3 \times 10^{12} \text{ m}^{-2}$  is adopted in estimating the value of  $-(m/\rho)(\partial\rho/\partial\varepsilon_{\text{pl,cum}})$  in equation (21).  $b$  is  $2.86 \times 10^{-10} \text{ m}$ ,  $t_2$  is about  $10 \mu\text{m}$  (Li *et al.* 2000b), and  $d_c$  is assumed to be approximately the spacing between the walls of a PSB, or the walls of a labyrinth structure, or the spacing between veins, so its typical value is chosen as  $1 \mu\text{m}$  (Mughrabi *et al.* 1979).  $m = 0.7$  (Greenman *et al.* 1967). For most cases the formation of DBs starts at around several hundreds to a few thousand cycles (Gong *et al.* 1997, Li *et al.* 1999a, b, c). Here,  $N = 1500$  cycles is chosen in estimating the value of  $-(m/\rho)(\partial\rho/\partial\varepsilon_{\text{pl,cum}})$  in equation (21). The dislocation avalanche factor for  $[112]$  is 1.72 (see equation (22) and table 2); then the value of  $-(m/\rho)(\partial\rho/\partial\varepsilon_{\text{pl,cum}})$  in equation (21) is  $-0.296$ . As shown in the description of figure 6 in the text, the sum of the first two terms of equation (9) is 0.428 at 1000 cycles and 0.247 at 2000 cycles; therefore the DBs would start to form in between these two values, where the sum of these three terms becomes negative.

From equation (21) the dislocation avalanche factor (Lee and Duggan 1994, Li *et al.* 1994) can be formulated as

$$\lambda = \left( \frac{\cos \beta}{f(\mathbf{s})\Omega_p\Omega_s} \right)^{1/2} \quad (22)$$

Table 2. The dislocation avalanche factors in copper single crystals.

Orientation	Loading axis	$\beta$ (degrees)	$\Omega_p$	Secondary slip system	$\Omega_s$	$f(\mathbf{s})$	Avalanche factor $\lambda$	$1/\lambda$
1(13)	[001]	45	0.41	D4 ( $\bar{1}\bar{1}1$ )[101]	0.41	0.707	2.43	0.41
2	$\bar{1}$ [17]	37.6	0.45	C1 ( $\bar{1}\bar{1}1$ )[011]	0.45	1.58	1.57	0.64
3	$\bar{1}$ [12]	30	0.41	C1 ( $\bar{1}\bar{1}1$ )[011]	0.41	1.73	1.72	0.58
4	$\bar{2}$ [23]	30.9	0.36	C1 ( $\bar{1}\bar{1}1$ )[011]	0.36	1.71	1.96	0.51
5	$\bar{1}$ [11]	54.7	0.27	C1 ( $\bar{1}\bar{1}1$ )[011]	0.27	0.816	3.11	0.32
6	$\bar{2}$ [33]	41.1	0.37	B5 (111)[ $\bar{1}\bar{1}0$ ]	0.37	1.50	1.91	0.52
7	$\bar{1}$ [22]	45	0.41	B5 (111)[ $\bar{1}\bar{1}0$ ]	0.41	1.41	1.72	0.58
8	$\bar{2}$ [55]	47.6	0.42	B5 (111)[ $\bar{1}\bar{1}0$ ]	0.42	1.35	1.68	0.59
9	[011]	60	0.41	B5 (111)[ $\bar{1}\bar{1}0$ ]	0.41	1.0	1.72	0.58
10	[034]	55.6	0.46	A3 ( $\bar{1}\bar{1}1$ )[101] B5 (111)[ $\bar{1}\bar{1}0$ ]	0.46 0.34	$\infty$ 1.13	0 1.78	$\infty$ 0.56
11	[012]	50.7	0.49	A3 ( $\bar{1}\bar{1}1$ )[101] B5 (111)[ $\bar{1}\bar{1}0$ ]	0.49 0.24	$\infty$ 1.26	0 2.06	$\infty$ 0.48
12	[017]	45.5	0.46	A3 ( $\bar{1}\bar{1}1$ )[101] C1 ( $\bar{1}\bar{1}1$ )[011]	0.46 0.39	$\infty$ 1.26	0 1.67	$\infty$ 0.59
14	$\bar{1}$ [35]	44.2	0.49	A3 ( $\bar{1}\bar{1}1$ )[101] B5 (111)[ $\bar{1}\bar{1}0$ ]	0.42 0.33	$\infty$ 1.43	0 1.76	$\infty$ 0.57
15	$\bar{5}$ [1 220]	42.2	0.48	A3 ( $\bar{1}\bar{1}1$ )[101] B5 (111)[ $\bar{1}\bar{1}0$ ]	0.40 0.33	$\infty$ 1.48	0 1.78	$\infty$ 0.56
16	$\bar{4}$ [1 841]	44.9	0.50	A3 ( $\bar{1}\bar{1}1$ )[101] C1 ( $\bar{1}\bar{1}1$ )[011]	0.47 0.32	$\infty$ 1.41	0 1.77	$\infty$ 0.56

The values of this factor calculated for various orientations are shown in table 2. In the calculation, the habit plane (101) of DBII is used in all cases except for the orientation [111], for which the habit plane (010) is used. On the [001]–[111] side of the standard stereographic triangle, the secondary slip system (111)[011](C1) with the maximum Schmid factor operates; on the [111]–[011] side, the secondary slip system (111)[110](B5) with the maximum Schmid factor operates. However, on the [011]–[001] side, if the secondary slip system (111)[101](A3) with the maximum Schmid factor operates, it cannot form DBs because  $\lambda = 0$ . On the other hand, if another slip system with the second largest Schmid factor operates locally, the DBs could be formed.

Generally speaking, during the process of the formation of DBs, the smaller the dislocation avalanche factor  $\lambda$ , the larger would be the plastic shear strain amplitude that is needed for the DBs formation. For multiple-slip single crystals,  $\lambda$  for the [011] orientation is smaller than for the [001] and [111] orientations (see table 2). This means that, for the orientation [011], a larger shear strain amplitude is needed to form DBs than for the other two orientations (see figure 1).

For comparison, the values of  $1/\lambda$  are shown in figure 9. If other conditions are identical, the greater  $1/\lambda$ , the larger is the plastic shear strain amplitude needed for the formation of DBs. The variation in  $1/\lambda$  with orientation is rather similar to the variation in the critical shear strain amplitude shown in figure 1. From these two figures, a better similarity can be found between the double- and multiple-slip single crystals. For example, along the sides of the stereographic triangle there are some wave crests in both figures, however, for single-slip single crystals, the values of  $1/\lambda$  are not as large as one might expect. This can be easily understood as follows. The driving force for the formation of DBs in single-slip single crystals is much smaller than in double- and multiple-slip single crystals as mentioned in § 3.3.2. Therefore the formation of DBs in single-slip crystals needs a much larger critical plastic shear strain than in the case of multiple- and double-slip crystals.

In this model, both primary and secondary slips operating in a local region were considered to account for the lattice rotation in the formation of DBs. DBI and

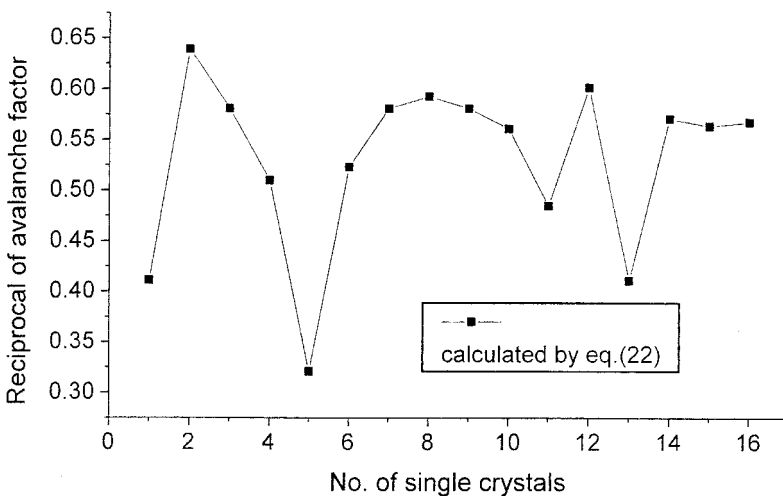


Figure 9. The variation in  $1/\lambda$  with the orientation of the single crystals.

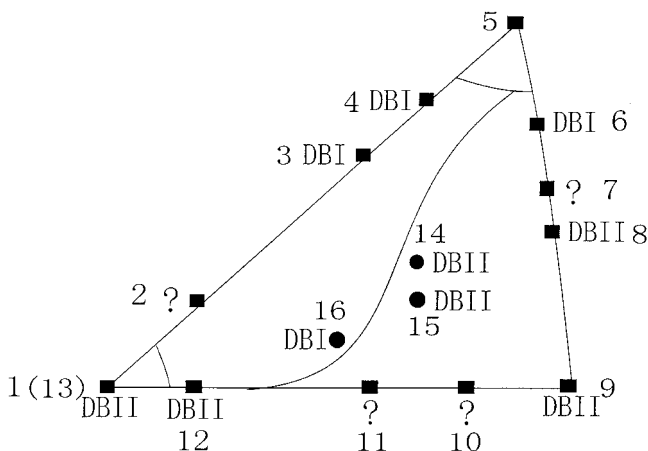


Figure 10. The types of DB first observed in the single crystals (Zhang 1995, Gong *et al.* 1997, Li *et al.* 1998b, 1999a, b, c).

DBII are expected to form simultaneously. However, the operation of a specific secondary slip system may be more favourable for stimulating one type of DB to appear on the sample surface markedly, and the other type of DB may not be observed clearly. If the applied strain amplitude is large enough, the other types of DB will appear prominently too. Figure 10 shows the types of DB observed first on the sample surface. From table 2, it seems that, in a single crystal in which the secondary slip system C1 operates, DBI will possibly be observed first and, when the secondary slip system B5 operates, DBII will be observed first. Therefore, the stereographic triangle may be divided mainly into two regions (figure 10). In region I, including orientations 2–4, 16 and 12, DBI is expected to be observed first while, in region II, including the orientations of 6–11, 14 and 15, DBII is expected to be observed first. This is in general accordance with the experimental observations except for orientation 12 in region I, and orientation 6 in region II. These two orientations are close to the highly symmetric multiple-slip [001] and [111] orientations respectively. The detailed reason for this inconsistency is unknown.

The formation of DBs in single crystals with various orientations is a general phenomenon in cyclic straining under constant plastic shear strain control. The formation of DBs in bicrystals has also been observed in the loading axis perpendicular (Zhang and Wang 1999) or parallel (Zhang *et al.* 1999) to the grain boundary. In polycrystals, the grains with various orientations in the plastic zone of a crack tip undergo cyclic straining. In this region, DBs formed within a grain have also been observed recently (Chen and Li 2002). All these experimental findings indicate that much work is still needed to understand the mechanisms for formation of DBs and their interactions with grain boundaries and triple junctions (Li *et al.* 2000a).

#### §4. SUMMARY

From the experimental results surveyed and the simple model proposed here, the formation of DBs in copper single crystals under cyclic straining might be understood as follows.

The loading axis rotation caused by tension and compression irreversibility is the major driving force for the formation of DBs. The drastically increasing mobile dislocation density caused by operation of secondary slip system locally is the direct trigger for the formation of DBs.

#### ACKNOWLEDGEMENTS

The work was financially supported by National Science Foundation of China under grants 59971058 and 59931020, and by the National Basic Research Project under grant G19990650.

#### APPENDIX A

From figure A1, the unit vector  $\mathbf{n}_z = \mathbf{n}_{\text{DBII}} \times \mathbf{L}$ , where  $\mathbf{n}_{\text{DBII}}$  and  $\mathbf{L}$  are the normal of DBII and the unit vector of loading axis respectively.  $\mathbf{n}_y = \mathbf{n}_z \times \mathbf{n}_{\text{DBII}}$ .

The coordinates  $(x_0, y_0, z_0)$  of O can be determined from

$$\mathbf{OC} = |\text{OC}| (\cos \beta \mathbf{n}_{\text{DBII}} + \sin \beta \mathbf{n}_y). \quad (\text{A } 1)$$

The unit vector of the secondary slip direction is  $\mathbf{s} = (s_1, s_2, s_3)$ . The secondary slip direction intersects the boundaries of DBII at O and B. The line that passes O and along  $\mathbf{s}$  can be expressed as

$$\frac{x - x_0}{s_1} = \frac{y - y_0}{s_2} = \frac{z - z_0}{s_3}. \quad (\text{A } 2)$$

The plane of  $yCz$  (one of the boundaries of DBII) is represented by

$$\mathbf{r} \cdot \mathbf{n}_{\text{DBII}} = 0. \quad (\text{A } 3)$$

From equations (A 2) and (A 3), the coordinates of B can be determined, and also the length of OB. Then the ratio  $f(\mathbf{s}) = |\text{OB}/\text{OC}|$  can be determined.

Figure A1. The geometry for the calculation of  $f(\mathbf{s})$ .

#### REFERENCES

- ANTONOPOULOS, J. G., BROWN, L. M., and WINTER, A. T., 1976, *Phil. Mag.*, **34**, 549.  
 ANTONOPOULOS, J. G., and WINTER, A. T., 1976, *Phil. Mag.*, **33**, 87.  
 BASINSKI, S. J., BASINSKI, Z. S., and HOWIE, A., 1969, *Phil. Mag.*, **19**, 899.  
 CHENG, A. S., and LAIRD, C., 1981, *Mater. Sci. Engng*, **51**, 111.

- CHEN, C. Q., and LI, S. X., 2002, *Acta mater.*, submitted.
- DILLAMORE, I. L., ROBERTS, J. G., and BUSH, A. C., 1979, *Metal Sci.*, **13**, 73.
- GONG, B., WANG, Z. G., and ZHANG, Y. W., 1995, *Mater. Sci. Engng*, **A149**, 171.
- GONG, B., WANG, Z. R., and WANG, Z. G., 1997, *Acta mater.*, **45**, 1365; 1998, *Mater. Sci. Engng*, **A245**, 55.
- GOSTELOW, C. R., 1971, *Metal. Sci. J.*, **5**, 177.
- GREENMAN, W. R., VREELAND, T. JR, and WOOD, D. S., 1967, *J. appl. Phys.*, **38**, 3597.
- HONG, S. I., and LAIRD, C., 1990, *Mater. Sci. Engng*, **A128**, 155.
- JIN, N. Y., and WINTER, A. T., 1984, *Acta metall.*, **32**, 989.
- KUHLMANN-WILSDORF, D., and LAIRD, C., 1977, *Mater. Sci. Engng*, **27**, 137, 1979, *ibid.*, **37**, 111.
- LEE, C. S., and DUGGAN, B. J., 1994, *Acta metall. mater.*, **42**, 857.
- LI, S. X., CHU, R. Q., HOU, J. Y., and WANG, Z. G., 1998a, *Phil. Mag. A*, **77**, 1081.
- LI, S. X., GONG, B., and WANG, Z. G., 1994, *Scripta metall. mater.*, **31**, 1729.
- LI, S. X., LI, Y., LI, G. Y., YANG, J. H., WANG, Z. G., and LU, K., 2002, *Phil. Mag. A*, **82**, 867.
- LI, S. X., REN, D. B., JIA, W. P., CHEN, C. R., LI, X. W., and WANG, Z. G., 2000, *Phil. Mag. A*, **80**, 1729.
- LI, X. W., WANG, Z. G., LI, G. Y., WU, S. D., and LI, S. X., 1998b, *Acta mater.*, **46**, 4497.
- LI, X. W., WANG, Z. G., and LI, S. X., 1999a, *Mater. Sci. Engng*, **A260**, 132, 1999b, *ibid.*, **A265**, 18, 1999c, *ibid.*, **A269**, 166; 2000b, *Phil. Mag. A*, **80**, 1901; 2000c, *Phil. Mag. Lett.*, **79**, 715, 2000d, *ibid.*, **79**, 869.
- LI, X. W., ZHANG, Z. F., WANG, Z. G., LI, S. X., and UMARKOSHI, Y., 2001, *Defects and Diffusion Forum*, **188–190**, 153.
- MUGHRABI, H., 1978, *Mater. Sci. Engng*, **33**, 207.
- MUGHRABI, H., ACKERMANN, F., and HERZ, K., 1979, *Fatigue Mechanisms*, ASTM Special Technical Publication 675 (Philadelphia, Pennsylvania: American Society for Testing and Materials), p. 69.
- REID, C. N., 1973, *Deformation Geometry for Materials Scientists* (Oxford: Pergamon).
- SALETORRE, M., and TAGGART, R., 1978, *Mater. Sci. Engng*, **36**, 259.
- VILLECHAISE, P., MENDEZ, J., and VIOLAN, P., 1991, *Acta metall. mater.*, **39**, 1683.
- YANG, J. H., LI, Y., LI, S. X., MA, C. X., and LI, G. Y., 2001, *Mater. Sci. Engng*, **A299**, 51.
- ZHAI, T., MARTIN, J. W., and BRIGGS, G. A. D., 1995, *Acta metall. mater.*, **43**, 3813.
- ZHAI, T., MARTIN, J. W., BRIGGS, G. A. D., and WILLKINSON, A. J., 1996, *Acta metall. mater.*, **44**, 3477.
- ZHANG, Y. W., 1995, Master's Thesis, Institute of Metal Research, Chinese Academy of Sciences.
- ZHANG, Z. F., and WANG, Z. G., 1999, *Phil. Mag. A*, **79**, 741.
- ZHANG, Z. F., WANG, Z. G., and HU, Y. M., 1999, *Mater. Sci. Engng*, **A272**, 410.
- ZHANG, Z. F., WANG, Z. G., and LI, S. X., 2000, *Phil. Mag. Lett.*, **80**, 525.

Copyright of Philosophical Magazine A is the property of Taylor & Francis Ltd and its content may not be copied or emailed to multiple sites or posted to a listserv without the copyright holder's express written permission. However, users may print, download, or email articles for individual use.